NEW ASPECTS OF EXCITATION AND PROPAGATION OF SUBSURFACE LONGITUDINAL AND TRANSVERS WAVES

A.R. BAEV, M.V. ASADCHAYA, G.E. KONOVALOV

SSI "Institute of Applied Physics of the Ac. Sci. Belarus", Minsk, Belarus

Introduction.

Subsurface waves (SW) - longitudinal (SL) and vertically polarized transverse (ST) waves excited at critical angles of incidence β_i an ultrasonic beam find increasing application in ultrasonic inspection [1-4], where β_i=arcsin(C_w/C_s), C_w and C_s is the velocity in acoustical line (wedge) and of the investigated medium, respectively; $s=l$ and $s=t$ correspond to longitudinal and transverse vibration modes. There are three basic ways of SW application: a) for detection and identifying subsurface discontinuities in articles with coarsely finished surface, for determining the of cracks depth; b) for structural spectroscopy and acoustic strain gauging; c) for measuring the solid acoustical properties.

Some features of SL and ST field formation have been investigated in works [1, 5-8], where the laws of SW directivity characteristic $\Phi(\gamma,\alpha)$ and amplitude P varying vs. the solid curvature, state of contact surface and etc. have been investigated. Partially, it was shown that directivity of longitudinal waves $\Phi(\alpha)$ reaches the maximum at angle 75-78° and transverse waves - aт angle 73-75°. Acoustical field of subsurface waves have complicated structure, and different laws of wave propagating nearly contact surface (z=0) and far enough from it ($z>>\lambda_s$). In the first case SL mode is attenuating with distance in far-zone like $\sim x^{-m}$, where n≈1,7-1,8 ([9]) and m=2 [5]. Experimentally determined coefficient n for ST mode is ~2,1-2,2 [6]. In the second case n=1. It is interesting that a trajectory of vector $\vec{\xi}(z,x)$ describing wave material particle displacement nearly contact surface is like elliptical; varying vs. distance x. If the upper medium or layer is a solid then both longitudinal and transverse vibrations can propagate in to it at an angle $\arcsin(C_{l_1}/C_{l_2})$ or $\arcsin(C_{t_1}/C_{l_2})$ respectively. It is clearly that the acoustical and geometrical properties of the upper layer may influence the phase and amplitude parameters of an acoustical signal when we have to solve the former problems - (a), (b), (c). The same problems arise when the form of a test object is not simple and there are conditions for appearance of "edge" and accompanied modes. Taking into account the wide possibilities from the previous type of wave application and real output problems, we could conclude that it is necessary to study the laws of SL and ST mode excitation and propagation in the solids of different geometric and boundary conditions at the interface surface. In this work we study, predominantly, peculiarities of SW excitation and propagation in solids with protective layer and with projection.

1. Features of SW propagation in solids with protective layer (PL).

1.1. Case $h>\lambda_p$. There are many articles covered by protective (technological) layer which necessary to inspect and solve problems (a-c) mentioned above. Subsurface wave diffraction effects can be used to define thickness and sound velocity under protective layer, which most often correlates well with physical and mechanical and structural properties of the base. There is dependence of SW time propagation between a pare of receiving probes with acoustical base L - $\Delta\tau$ *(h, C_p, C_s, L)* using which it is possible to find sound velocities C_p in materials or the layer thickness; $C_p=L/\Delta\tau$, if h=const. But if $h\neq$ const – it is necessary make additive "sounding of the object" by changing the direction of sounding. In this case we have two equations to define C_p more exactly.

Let ultrasonic arrangement consist of four probes and set on the solid with protective layer which sound velocity $C_p>C_s$ and thickness $h>\lambda_p$. Fig.1 illustrates the method of ultrasonic determination of physico-mechanical properties of the solid base by using data on SW time propagation $\Delta\tau_i$ from transmitting probes (1, 2) to receiving probes (3,4), when protective layer is thick and have varying thickness h. The scheme of ultrasonic sounding: a) probe 1→ probe 3 and 4 (i=1); b) probe 2→

probe 4 and 3 (i=2). So, formula for C_s is

$$C_s = C_{s0}\{1 - 0{,}5n_{ps}(\Delta\tau_0)^2 + 0{,}0625n_{ps}^2(\Delta\tau_0)^4 - 0{,}25n_{ps}^4(\Delta\tau_0)^8\}, \quad (1)$$

where $C_{s0}=2L(\Delta\tau_1+\Delta\tau_2)^{-1}$, $\Delta\tau_o=(\Delta\tau_1-\Delta\tau_2)(\Delta\tau_1+\Delta\tau_2)^{-1}$, $n_{ps}=C_p/C_s$.

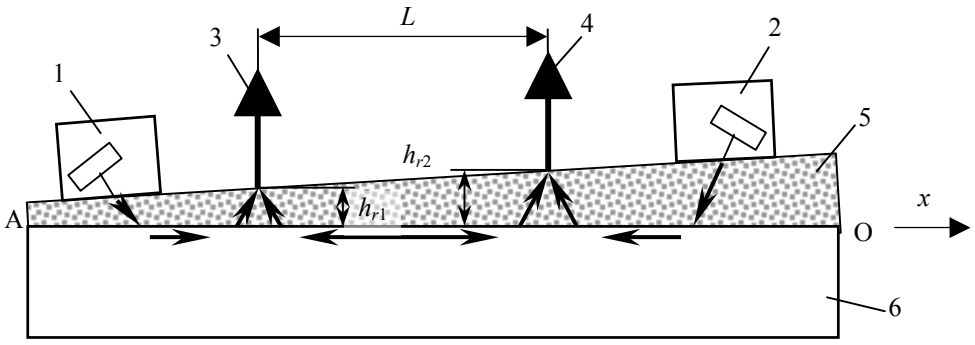

Fig.1. Scheme of ultrasonic method determination of acoustical and physico-mechanical properties of double-layer materials: 1, 2 – transmitting probes; 3, 4 – receiving probes; 5 – protective layer; 6– the object of testing

1.2. Case $h\sim\lambda_p$. Interference phenomena arise when the SW modes are exciting and propagating nearly interface boundary protective layer base. The protective layer of $h^*=h/\lambda_p$ thickness under the probe-emitter (or receiver) can be considered as additive resonance "wave guide element" with wavelength λ_p. To reveal the opportunities of leveling the interference effect influence, we carried out experimental studies according to conventional technique [6]. To make research, an enamel coating with 0,1 mm pitch was applied to the steel specimen surfaces, a cylindrical reflector being made in metal and its axis parallel to contacting plane. Duet scheme of sounding was used and exit angle in the steel base of the specimen was $\alpha_m = arcsin(C_w/C_p)\approx$14-15°. We have obtained dependencies of the echo-signal amplitude P vs. PL thickness at wave frequency 1,8 MHz.

As there show, amplitude function $P(h^*)$ is oscillating one, and amplitude variation can be from 7-8 dB up to ~10-12 dB. The method of the acoustical path stabilization when interference phenomena in protection layer to be appear has been developed. To diminish oscillation of P vs. h^* we suggest to use the additive acoustical echo-canal (path), created by normal probe installed in a common corps and its amplitude of reflected mode $P_0 \sim P_{SW}$ if the optimal wave frequency ν_{ad} determined from the derived formula

$$\nu_{ad}\approx\frac{C_{pl}}{C_s[1-n_{ps}^2(\sin\alpha_m)^2)}. \quad (2)$$

(It is necessary to satisfy requirement of the phases shifts $\Delta\vartheta$ equality appearing in the result of the modes re-reflection between solid base and wedge.)

It should be noted that if SW probes set on the protective layer and used to determine amplitude P or velocity C_s dependences vs. material characteristics of the solid base there are can be appear two types of interference: the first one was mentioned above but the second one is caused by wave re-reflection in the protective layer between probes when SW propagating along interface. This process illustrates Fig.2 in which modeling layer is fluid. It was revealed, that the pulse function $P(h^*)$ can be varying up to 10 dB and more if a ratio of the acoustical impedances (solid base-fluid) is lesser or about 10 and the layer opposite surface is free or rigid. In such conditions we observe substantial pulse deformation that plays parasitic role when time measuring. Note, that this effect can be used to measure physico-mechanical properties of subsurface properties of solids.

2. Features of SW propagation in solids with step projection and fillet transition (FT).

Some results of SW propagation in objects with step projection have been published in works [6]. It was discovered that ST-wave probe excite the base and the surface modes which amplitudes are

simile to each other. Surface mode transformed into volume transverse one interacts with the base mode changing the resulting field. Therefore, firstly, we decided to make detail analysis and experimentally study the features of the surface (Rayleigh**)** waves transformation into the volume or edge modes at the fillet transition of projection. The common illustration and the problem to consider in our work are in Fig.3.

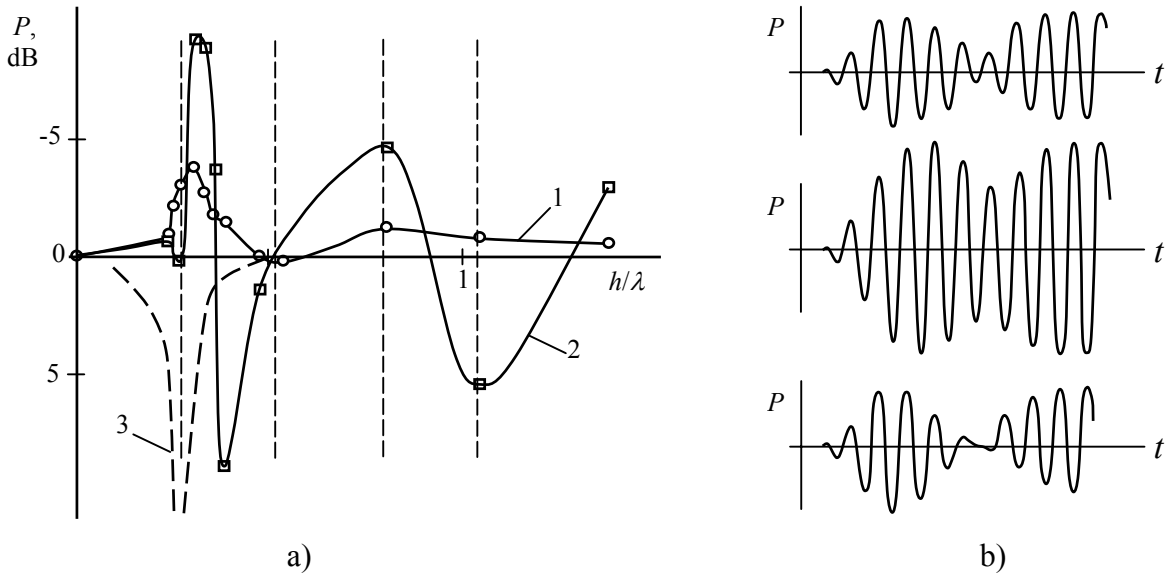

Fig.2. Amplitude of SL (1,2) and RW (3) and the pulse forms vs. fluid thickness: contacting materials: Aluminum-Oil

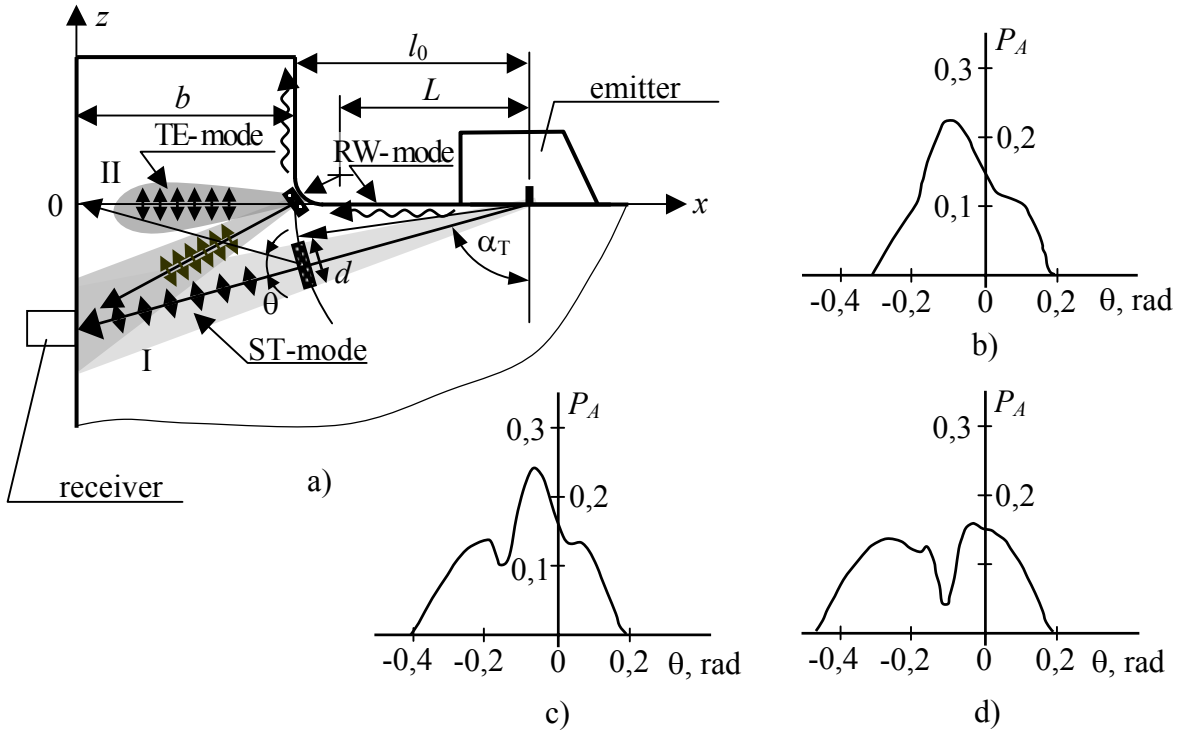

Fig.3. Illustration and physical model of an acoustical field formation with projection and fillet (a) and dependences P vs. angle θ (b-d); the phase shift between ST and RW mode $\Delta\Psi_{SR} = 0{,}7\pi$ (b); $1{,}8\pi$ (c); $2{,}7\pi$ (d)

2.1. Experimental techniques. Experimental techniques are clarified in the corresponding figures (Figs. 4–11). Units of a standard acoustic flaw detector have been used as a source and amplifier of the probe signal. The signal's amplitude was measured by comparing it to the reference signal of a signal generator displayed on an oscilloscope screen. External synchronization, delay, and sweep of the signal were provided and its time characteristics were measured using an I2-26 device. Undetected probe signals were used in the study, enabling an increase, owing to a specific feature of the equipment operation, in the accuracy of the measuring system. The directivity characteristic of the source of ultrasonic vibrations in the incidence plane was determined using well-known recommendations [9]. The transverse mode was detected by an electromagnetic–acoustic (EMA) receiver. The width of the solenoid's winding determines the dimensions of the zone where vibrations can be detected; in the case considered, it is 0,0015 m. The localized high-strength field in the zone of EMA detection was created by closing the magnetic flux from the pole of a Sm–Co magnet with a steel plate whose front face contacts the solenoid's coils through a thin insulating plate. A 0,002-m-wide and 0,01-m-long normal piezoelectric probe was used as a detector of longitudinal vibrations. Predominantly, Steel specimens with FT of different curvature (0-9 mm) and width (53, 37, 14 mm) of projection were used as the objects of research.

2.2. Peculiarities of the Rayleigh wave excitation and transformation at the fillet transition of projection. The peculiarities of an acoustical field formation in an object with a projection have been revealed as a function of a curvature radius of a fillet transition, Rayleigh wavelength λ_R, distance between probe and fillet transition (FT) of projection. (The base experimental data are in Fig.4-11). Neglecting divergence and energy dissipation of surface wave propagating along contact surface the law of the acoustical energy conservation can be written

$$K_{ref} + K_{trans} + K_{prop} = 1, \qquad (3)$$

where K_{ref}, K_{trans} and K_{prop} – are the coefficients of the acoustical energy reflection, transformation and propagation through FT of different curvature r^{-1}.

Note, that according to [8] if $r^* = r/\lambda_R >> 1$ the surface wave, propagating through FT, loses energy by radiating edge transverse P_{TE} and longitudinal P_{LE} waves normally to the fillet transition surface. So it is possible to write: $\mathrm{d}\vec{W}_{TE} = \vec{C}_T U_{TE}\, dl$, $\mathrm{d}\vec{W}_{LE} = \vec{C}_L U_{LE}\, dl$, where U_{TE} and U_{LE} - are the "middle" energy densities of the edge transverse and longitudinal mode properly; $dl = r d\theta$. Using the energy balance law and some assumptions ($\widetilde{U}_R \sim (P_R)^2$, $U_{TE} \sim (P_{TE})^2$, $U_{LE} \sim (P_{LE})^2$) an equation derived to evaluate amplitude of the edge transverse wave P_{TE} is

$$P_{TE} \approx P_{LE}/\varepsilon n_R \sim P_{R0} \sqrt{\frac{2\gamma}{m_R + n_R \varepsilon}}\, (\gamma)^{1/2} exp[-r_\lambda (\gamma - i)\, \theta + \Delta\phi], \qquad (4)$$

where γ - is an attenuation coefficient of RW-mode per λ_R, depending on $r_\lambda = r/\lambda_R$ (predominantly) and Poisson coefficient (weakly); $m_R = \frac{C_T}{C_R}$; $n_R = \frac{C_L}{C_T}$; $\varepsilon = W_{TE}/W_{LE}$; $\Delta\phi$ - "a possible" constant phase shift when the elementary part of FT surface dl re-radiates edge wave. So it is possible to conclude, that FT surface is "a special ultrasonic erial" with amplitude and phase distribution vs. angle θ between radius-vector $\vec{r}$ and the normal to contact surface. If $\theta = 0$ $P_R = P_{R0}$, $\theta = \pi/2$ - $P_R = P_{R0}\, exp\, [-r_\lambda (\gamma - i)\, \frac{\pi}{2} + \Delta\phi]$. So, equation (4) can be used to evaluate acoustical field of TE mode in projection with curvilinear FT if $r_\lambda > 5$-10.

According to theoretical [8] and our experimental data (Fig.4) the more the r_λ the smaller the amplitude of the edge waves, where $P_{TE}/P_{LE} > 10$. (So, it is possible to neglect the part energy W_{LE} caused by transformation RW$\rightarrow W_{LE}$ at the fillet transition). But from another side – the effective aperture of the former "emitter" and time (or the phase shift $\sim \Delta\theta\, r_\lambda$) delay between points on the FT surface at different angles θ_i are increasing function vs. r. The former factors may influence

substantially acoustical field in the volume of projection.
In reality when r_λ is varying from 0 up to 5-10 the numerical data of theory is not correct and it is necessary to obtain experimental data. The peculiarities of an acoustical field formation in an object with a projection have been revealed as a function of a curvature radius of a fillet transition and Rayleigh wavelength λ_R.

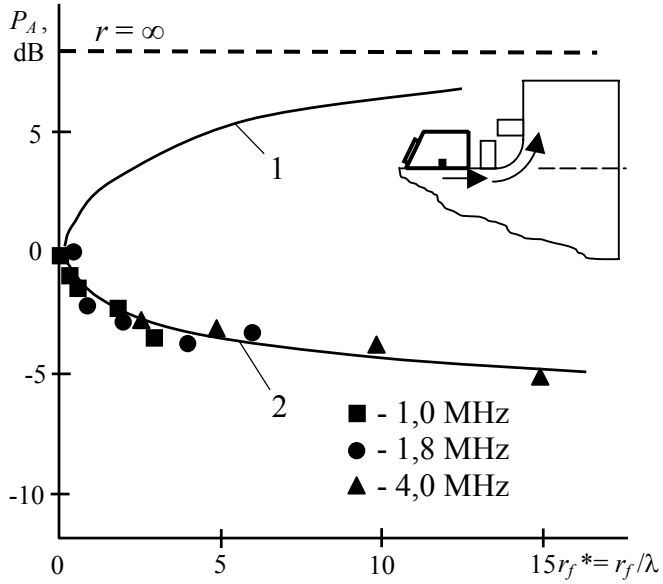

Fig.4 – Rayleigh wave amplitude transmitted through fillet transitions (1) and amplitude of the STV mode, transformed of Rayleigh wave at fillet transition (2): □, ○, Δ - experimental date

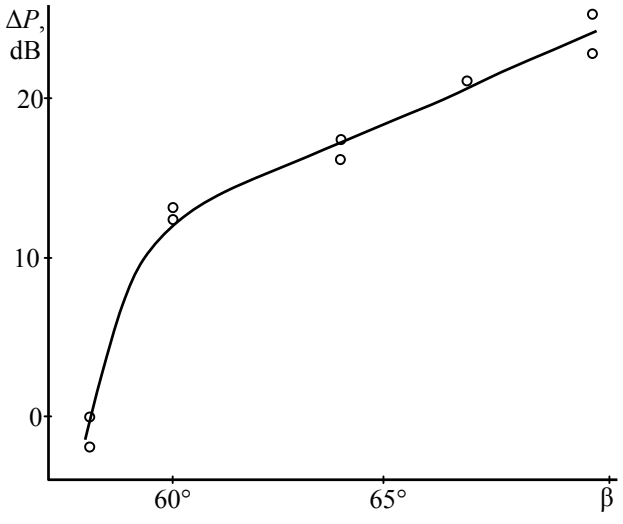

Fig.5. Experimental data of $\Delta P = P_{RW}/P_{ST}$ vs. wedge angle β: frequency 1 MHz; acoustical base or distance to receiver ≈55 mm

It should be noted, that RW excitation is accompanied by appearance of the ST mode which amplitude behavior vs. wedge angle β is simile like in Fig.5: ν=1 MHz and distance from the probe to receiver ≈55 mm. As our experiments show (Fig.6) the field of the "secondary" ST wave "takes active part" to form the resulting field in the projection volume when the probe position is close to FT and vice versa – the more the distance to FT the smaller the ratio $P_{SE} = P_{TS}/P_{TE}$.
This effect depends too vs.: frequency varying of the phase shift ΔΨ between the former modes

$$\Psi = 2\pi \nu \Delta x \,(1/C_R - 1/C_T) + \Delta\Psi,$$

where ΔΨ - the phase angle to appear in the result of the waves excitation and transformation at FT; angle between RW wave vector $\vec{k}_R$ and the axe y (Fig.7 illustrates varying of the amplitude of RW reflected from FT vs. ψ for r_λ <<1). As there are show, if the angle ψ is not more 20-30° than it is possible to neglect by the coefficient K_{ref} in equation (3) for every r_λ . But the RW reflection coefficient increases significantly with ψ→50-60° and more. It is interesting, that the angle of TE and TS propagation in the projection volume does note coincide with ψ.
An example of the acoustical field formation in the projection specimen with the FT of different radius r_λ and the wedge angle β=64° is in Fig.6. It is evidently, that additive field,

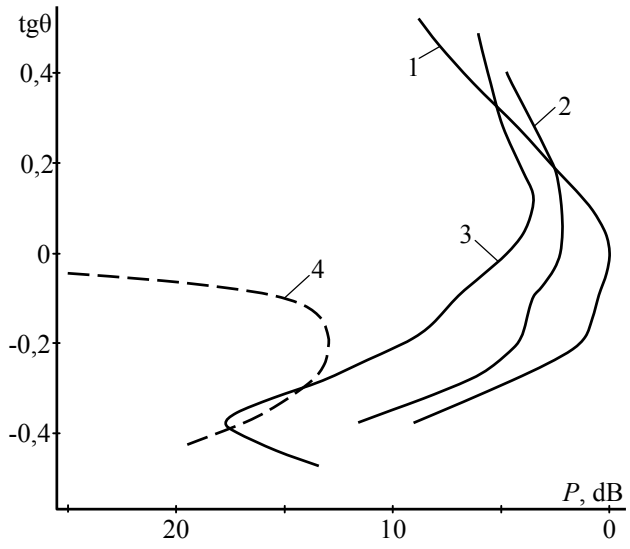

Fig.6. Acoustical field of the ST-probe in the specimen with projection vs. r_λ: r_λ = 0 (1); 1,8 (2); 5,5 (3); ∞ (4); ν=1,8 MHz; β=64°

created by TS mode occur influence on the resulting field form. And in this case we observe the maximum of $P(\phi)$ shift in z positive direction and the width directivity growth for $z<0$.

The data in Fig.8 obtained for amplitude dependences $P(z)$ of the signal reflected from the cylindrical reflectors in projection show noticeable varying of the method ability to detect artificial defects vs. distance to FT when RW-probe works in echo-regime. So, if the probe is close to FT its an "effective directivity" is forming by P_{TE} and P_{TS} and have maximum $P_{SE} = P_{TS} / P_{TE}$ as well as maximum of the effective aperture D of the former imaginary acoustical sources. Magnitudes of the P_{SE} and D vs. x_0 are decreasing function vs. x_0, that naturally causes the width growth of the normalized function $P(z)$ at $z<0$.

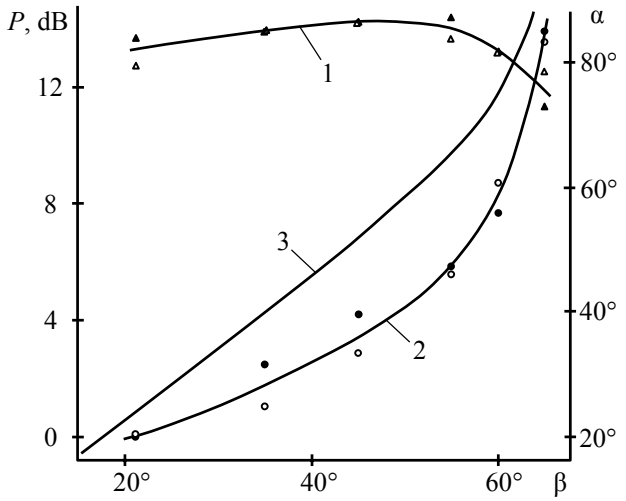

Fig.7. Amplitude of RW reflected from FT (1) and rectangular cone (2) and direction angle of TE propagation in the projection volume (3)

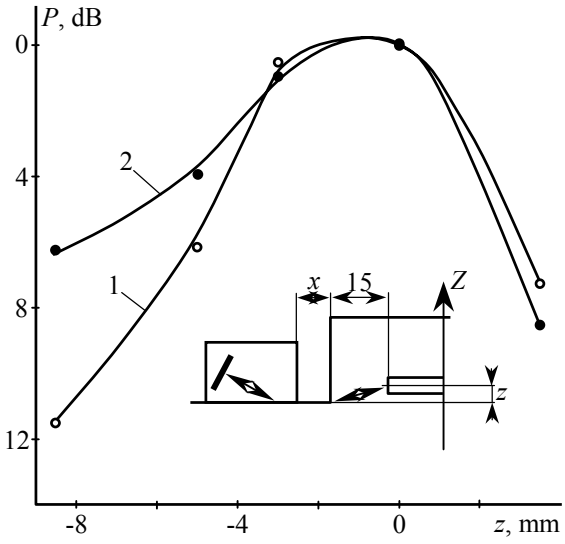

Fig.8. Amplitude of TE-mode reflected from the plane surface of cylindrical reflector made in projection vs. reflector′s z-position: distance from the probe to FT x, mm = 0 (1); 30 (2)

It can be explained by the next factors: limited time duration of the pulse; small distance from the reflected surface of artificial flaw to internal vertical plane of the projection.

2.3. Features of the ST vertical and SL wave field formation in solid with the step projection and fillet transition. During another set of measurements we have investigated the acoustical fields of SL probes. Fig. 9 demonstrates classical effect of SL wave diffraction in the projection with transition fillet where the modes transformation (as above mentioned) absent. As seen Fig.9, a width of normalized $P(\phi)$ is increasing function vs. FT radius and its growth achieves up to 25-30 % for r_λ increasing from 0 to ∞. But as for the acoustical fields of ST probe in the solid projection there is another situation.

As seen Fig.10, ST wave emitter probe excite in solids subsurface and surface waves of the simile amplitude at the incidence angle of $\beta \approx arcsin(C_p/C_T)$. As experiment show we found different "pictures" of the $P(z)$ distribution vs. distance from the probe to the fillet transition and frequency ν, including two or more peaks and their displacement along z. The simplified physical model of the acoustical two-dimensional field formation of ST wave emitter probe in solids with a step projection (or with small radius of the fillet transition r_λ <0,5) is developed. It is based on the representation of $\Phi(\alpha)$ as a superposition of the fields of two coherent sources: the principal mode (Φ_{TS}) and the secondary mode transformed at the fillet transition from the accompanying Rayleigh wave - Φ_{TE}.

We assume: the acoustical source of Φ_{TE} is a straight line coinciding with the coordinates {y=0, z=0, x=x_0}; the second acoustical source of Φ_{TS} is describing by the function ~$d\cos\Xi(\alpha-\alpha_m)$, where d – is the source′s aperture taken at the level of ~6 dB and Ξ - constant. We also took into account

the form of the pulse and its duration. The experimental data have been obtained for frequency ν=1,8 MHz.

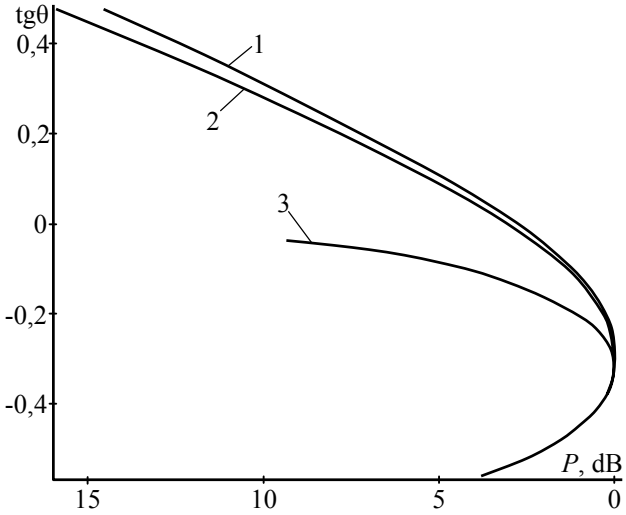

Fig.9. Acoustical field of LW-probe in the specimen with projection (1, 2) and without it (3): r_λ = 0 (1); 2,7 (2)

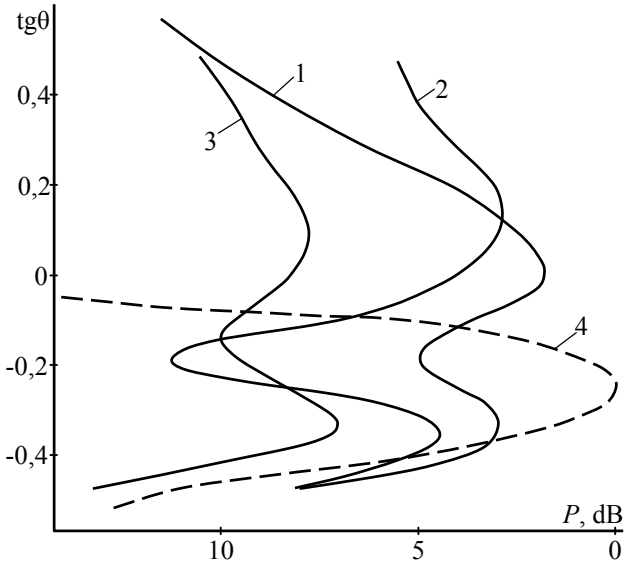

Fig.10. Acoustical field of the ST-probe in the specimen with projection (1-3) and without it (4): r_λ=0 (1); 1,7 (2); 5 (3); β=58°

Some data of the $\Phi(\phi)$ calculations vs. the phase shift Ψ between ST and RW mode or caused by the probe position changing along *x* are in Fig.3. As our laboratory finding and numerical data show the phase shift Ψ between principal ST mode and RW one transformed into the transverse volume mode (TE) causes more substantial $\Phi(\phi)$ changing. The numerical data of the suggested model calculations (Fig.11) demonstrate a good qualitative agreement with the experimental data. (To diminish the divergence between numerical and experimental data it is necessary, firstly, to imagine more exactly the theory model of RW→TE transformation for r_λ<5).

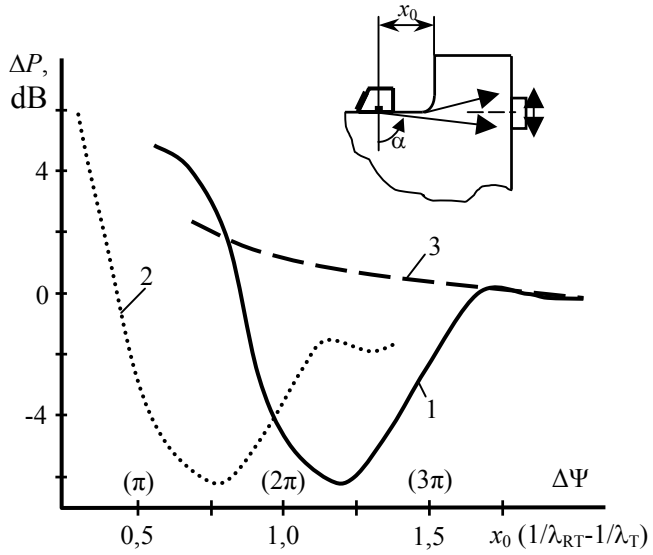

Fig.11. Experimental (1, 3) and theoretical (2) parameters of an acoustical field of the ST-probe in the rectangular projection vs. distance to FT that is accompanied by varying of the phase shift between the "model sources" of the *ST* and *TE* modes: $\Delta P_{u,d}=(P_u)_{max}/(P_d)_{max}$: maximum amplitude of $P_u(z>0)$ and P_d $(z<0)$; r_λ = 0 (1, 2); ∞ (3)

So, it is possible to control acoustical fields created by ST vertically polarization V probes in the solid projections by varying the next parameters of inspection: distance from the probe to the fillet transition; frequency ν; wedge angle β; direction of the probe incidence plane in regard to FT generatix. Sometimes it is possible to damp RW mode and to control the acoustical field directivity by the fluid layer (including magnetic fluid posed in magnetic field [10]) put on the contact surface.

In the some cases the probes with wedge angle $arcsin(C_p/C_R)$ can be independently used to detect flaws including "slipping" posed in the projection volume nearly imaginary plane coinciding with the contact plane.

It was shown too that sometimes it is possible to inspect the former objects by using RW probes and TE mode transformed at the fillet transition simultaneously. The projection inclination to contact surface of

the object causes K_R, K_{RT} and $\Phi(\alpha)$ varying vs. an angle inclination.

This material is based upon work, supported by Byelorussian Fond of Foundation Research.

References

1. Ermolov, I.N., Razygraev, N.P., and Shcherbinskii, V.G. Study of the Process of Formation of a Head-Wave Acoustic Field in a Monitored Medium, Defektoskopiya, 1978, no. 11, pp. 5–10.
2. Razygraev, N.P. On Detecting Subsurface Flaws Using ИЦ-61 and ИЦ-70 Head Wave Selectors, Defektoskopiya, 1981, no. 3, pp. 97–100.
3. Brokowski, A., Deputat, J., and Mizerski, K. Method of Measurement of Residual Stresses in the Material of the Object under Test, US Patent 4 926 692, MKI G01N 29/00, 1990.
4. Baev, A.P., Konovalov, G.E., Mayorov, A.L., Asadchaya, M.V., and Tishchenko, M.A. Methods of Detecting Discontinuity Flaws and Inspection of Cast Iron Structure Using Body and Head Waves, Lit'e Metal., 2004, no. 4, pp. 95–100.
5. Brekhovskikh, L. M. Waves in layered media. London, New York:Academic Press, 1960, 511 p.
6. Bayev, A. R., and Asadchaya, M. V. Specific Features of Excitation and Propagation of Longitudinal and Transverse Subsurface Waves in Solids: I. Waves in Objects with a Free Plane Boundary, Russian Journal of Nondestructive Testing, Vol. 41, No. 9, 2005, pp. 567–576.
7. Nikiforov, L.A. and Kharitonov, A.V. Parameters of Subsurface Longitudinal Waves Excited by Wedge-Type Transducers, Defektoskopiya, 1981, no. 6, pp. 80–85.
8. Viktorov, I.A. Zvukovye poverkhnostnye volny v tverdykh telakh (Surface Acoustic Waves in Solids), Moscow: Nauka, 1981.
9. Non-Destructive Testing: Reference book of 7 vol. / Edited by V. V. Kluev. V.3. Ermolov I. N., Lunge Y. V. Ultrasonic inspection. – M.: Mashinostroenie, 2004.
10. Baev, A.P., Konovalov, G.E., and Maiorov, A.L. Magnitnye zhidkosti v tekhnicheskoi akustike i nerazrushayushchem kontrole (Magnetic Liquids in Technical Acoustics and Nondestructive Testing), Prokhorenko, P.P., Ed., Minsk: Tekhnalogiya, 1999. – 256 p.